Deep-Sea Research II 57 (2010) 1433–1445

Contents lists available at ScienceDirect

Deep-Sea Research II

journal homepage: www.elsevier.com/locate/dsr2

Dissolved organic carbon export and subsequent remineralization in the mesopelagic and bathypelagic realms of the North Atlantic basin

Craig A. Carlson [a,*], Dennis A. Hansell [b], Norman B. Nelson [c], David A. Siegel [c,d], William M. Smethie [e], Samar Khatiwala [e], Meredith M. Meyers [a], Elisa Halewood [a]

[a] Ecology, Evolution, and Marine Biology, University of California, Santa Barbara, CA 93106
[b] Rosenstiel School of Marine and Atmospheric Science, University of Miami, Florida, 33149
[c] Institute for Computational Earth System Science, Mail Code 3060, University of California, Santa Barbara, CA 93106
[d] Department of Geography, University of California, Santa Barbara, CA 93106
[e] Lamont-Doherty Earth Observatory of Columbia University, Palisades, NY

ARTICLE INFO

Article history:
Received 7 May 2009
Accepted 1 December 2009
Available online 7 March 2010

Keywords:
DOC
CFC
AOU
Carbon export
NADW

ABSTRACT

Dissolved organic carbon (DOC) data are presented from three meridional transects conducted in the North Atlantic as part of the US Climate Variability (CLIVAR) Repeat Hydrography program in 2003. The hydrographic sections covered a latitudinal range of 6°S to 63°N along longitudes 20°W (CLIVAR line A16), 52°W (A20) and 66°W (A22). Over 3700 individual measurements reveal unprecedented detail in the DOC distribution and systematic variations in the mesopelagic and bathypelagic zones of the North Atlantic basin. Latitudinal gradients in DOC concentrations combined with published estimates of ventilation rates for the main thermocline and North Atlantic Deep Water (NADW) indicate a net DOC export rate of 0.081 Pg C yr^{-1} from the epipelagic zone into the mesopelagic and bathypelagic zones. Model II regression and multiple linear regression models applied to pairwise measures of DOC and chlorofluorocarbon (CFC-12) ventilation age, retrieved from major water masses within the main thermocline and NADW, indicate decay rates for exported DOC ranging from 0.13 to 0.94 μmol kg^{-1} yr^{-1}, with higher DOC concentrations driving higher rates. The contribution of DOC oxidation to oxygen consumption ranged from 5 to 29% while mineralization of sinking biogenic particles drove the balance of the apparent oxygen utilization.

1. Introduction

Dissolved organic carbon (DOC) is the largest pool of organic matter in the ocean, yet it is only over the past decade that the oceanographic community has developed the analytical skill necessary to begin a reliable description and quantification of its contribution to the marine carbon cycle (Sharp et al., 2002). DOC plays an important role in the biogeochemistry of the ocean carbon cycle and can contribute to the biological pump (Copin-Montégut and Avril, 1993; Carlson et al., 1994; Hansell and Carlson, 2001a; Kähler and Koeve, 2001; Amon et al., 2003; Sohrin and Sempere, 2005). The export of sinking biogenic particles has long been known to drive respiration in the ocean interior and to help maintain the ocean's strong vertical gradients of inorganic carbon and nutrient concentrations. However, it is only recently that the contribution of DOC to carbon export and the maintenance of vertical gradients on biogeochemical properties have been recognized (Hansell and Carlson, 2001b).

DOC export from the surface ocean is a consequence of its accumulation in the euphotic zone, redistribution to higher latitudes with the wind-driven circulation, and eventual transport to depth with the overturning circulation at high latitudes and subduction in the subtropical gyres (Hansell, 2002). DOC contributes to the long-term sequestration (decades to centuries) of carbon via meridional overturning circulation resulting in ventilation of the deepest ocean layers. While observations show a 29% decrease in the deep-water DOC concentrations as it is transported via abyssal circulation from the North Atlantic to the North Pacific (Hansell and Carlson, 1998; Hansell et al., 2009), a detailed picture of the transport and decay of DOC along its pathways into the deep North Atlantic is still largely missing. Furthermore, the extent of DOC variability, the details of its export (amount and quality), and its rate of decay and contribution to apparent oxygen utilization (AOU) in the interior of the North Atlantic basin have yet to be detailed. These processes set the initial condition for further distribution of the exported DOC into the rest of the deep ocean via the global ocean "conveyor belt".

This lack of knowledge exists because of the paucity of high-quality DOC observations throughout the world oceans and from the North Atlantic in particular. In 2003, high quality and spatially

* Corresponding author. Tel.: +8058932541; fax +8058938062.
E-mail address: carlson@lifesci.ucsb.edu (C.A. Carlson).

0967-0645/$ - see front matter © 2010 Elsevier Ltd. All rights reserved.
doi:10.1016/j.dsr2.2010.02.013

expansive sampling of DOC was conducted in this basin as part of the Climate Variability (CLIVAR) Repeat Hydrography program (Feely et al., 2005). Here, we present recent DOC and hydrographic observations from three basin-scale meridional transects across the North Atlantic Ocean (i.e. CLIVAR lines A16N, A20, and A22). These data reveal the distribution patterns and dynamics of DOC as it is exported and transformed within the mesopelagic and bathypelagic zones of the North Atlantic basin. The DOC data, in combination with chlorofluorocarbon (CFC) ventilation ages and AOU tracers, were used to: (1) estimate DOC export and its contribution to total export production; (2) estimate the decay rates of exported DOC; and 3) determine the degree to which the oxidation of DOC contributes to AOU within the interior of the North Atlantic basin. The data confirm that DOC export by the Atlantic Ocean's meridional overturning circulation is an important component of the biological pump.

2. Methods

2.1. Study area

Data are presented from three meridional transects conducted in the North Atlantic as part of the US CLIVAR Repeat Hydrography program in 2003. The cruises were conducted aboard the NOAA Ship *Ronald H. Brown* (A16N; June–July 2003) and the *R.V. Knorr* (A20 and A22; October–November 2003), covering latitudinal ranges of 6°S to 63°N along longitude 20°–29°W (line A16N), 7°N–43°N along 52°W (line A20), and 11°N–40°N along 66°W (line A22) (Fig. 1). Hydrographic data were collected with a nominal station spacing of 50 km using a conductivity, temperature and depth (CTD) profiler equipped with 36 twelve-liter Niskin bottles.

2.2. Sample collection

Bottles were tripped throughout the entire water column (Feely et al., 2005). Hydrographic parameters included temperature, salinity, dissolved oxygen, and chlorofluorocarbon species (CFC-11, CFC-12 and CFC-113). WOCE standard protocols were used for all hydrographic measurements (WOCE operations manual, 1994; WHP91-1). Details of the measurement protocols, cruise narratives, and all data are available at the CLIVAR Repeat Hydrography Program website (http://cchdo.ucsd.edu/).

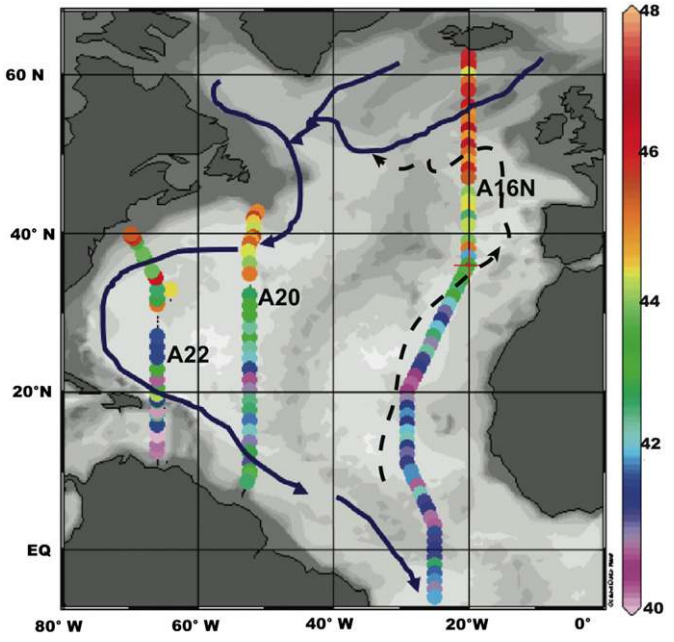

Fig. 1. Station map of meridional transects A16, A20 and A22 conducted as part of the US CLIVAR Repeat Hydrography project cruises in 2003. Color dots represent DOC concentration (μmol kg^{-1}) on the γ^n 27.9 kg m^{-3} surface (interpolated result using Ocean Data View; Schlitzer, 2004). The blue arrows indicate the generalized flow of NADW and the broken arrow represent slow water mass modification of AABW (Schmitz, 1996).

Table 1
Number of stations at which DOC profiles were determined and corresponding number of samples analyzed during the North Atlantic CLIVAR cruises conducted in 2003.

Cruise	Date	Latitudinal range	Number of stations	Number of measurements
A16	Jun–Aug 2003	63.3°N–6°S	73	2050
A20	Sep–Oct 2003	43.2°N–7°N	33	784
A22	Oct–Nov 2003	40°N–11.3°N	43	894

More than 3700 DOC samples were collected from 150 profiles along the three transects (Table 1). DOC concentrations were determined from the same bottles from which CFC and oxygen were collected. DOC samples were collected from approximately every other CTD cast (i.e., horizontal spacing of ~100 km) and sampled from 24–36 depths. Samples from the surface down to 1000 m (or upper 250 m on A16N) were passed through an inline polycarbonate filter cartridge holding a combusted GF/F filter attached directly to the Niskin bottle. Previous work has demonstrated that there is no resolvable difference between filtered and unfiltered samples in waters below 1000 m at the μmol kg^{-1} resolution (Hansell and Carlson, 2001a). Water was dripped directly into high-density polyethylene bottles that had been acid leached, flushed with Nanopure® water and dried prior to each cruise. The samples were stored frozen at −20 °C in volatile organic-free freezers until analysis at shore-based laboratories at the University of California, Santa Barbara (UCSB) and the University of Miami.

2.3. DOC analysis

All samples were analyzed via high-temperature combustion on Shimadzu TOC-V analyzers that were slightly modified from the manufacturer's model system. The condensation coil was removed and the head space of an internal water trap was reduced to minimize system dead space. The combustion tube contained 0.5 cm Pt pillows placed on top of Pt alumina beads to improve peak shape and to reduce alteration of the combustion matrix throughout the analytical run. CO_2-free carrier gas was delivered to the TOC-V systems via commercial ultra high purity gas cylinders or a Whatman® gas generator. Three milliliters of sample were drawn into a 5 ml injection syringe, acidified with 2 M HCL (1.5%), and sparged for 1.5 min with CO_2-free gas. Three to five replicate 100 μl of sample were injected into the combustion tube heated to 680 °C. A magnesium perchlorate trap was added to the existing water and halide traps to ensure removal of water vapor from the gas line prior to entering a non-dispersive infrared detector. The resulting peak area was integrated with Shimadzu chromatographic software.

Extensive conditioning of the combustion tube with repeated injections of low carbon water (LCW) and deep seawater was essential to minimize the machine blanks. The system response was standardized daily with a four-point calibration curve of potassium hydrogen phthalate solution in LCW. Sample and reference swapping and intercalibration exercises were conducted periodically between the UCSB and University of Miami to ensure comparability between sample sets. All samples were

systematically referenced against low carbon water, deep Sargasso Sea reference waters (2600 m), and surface Sargasso Sea water every 6–8 analyses (Hansell and Carlson, 1998; Carlson et al., 2004). Daily reference waters were calibrated with DOC Consensus Reference Waters (Hansell, 2005). The standard deviation of the deep and surface references analyzed throughout a run generally had a coefficient of variation ranging between 1–2% over the 3–7 independent analyses (number of references depended on the size of the run), allowing resolution of approximately 1 μmol/kg in the deep waters.

2.4. CFC-derived ventilation ages

Chlorofluorocarbon concentrations (here, CFC-12), determined with a method similar to that described by Bullister and Weiss (1988), were used to estimate water mass ventilation ages of the waters (e.g. Doney and Bullister, 1992). As in Nelson et al. (2007), the partial pressures of CFC-12 (pCFC-12) required to produce the measured CFC-12 concentrations were computed as the quotient of the CFC-12 concentrations and the solubility constant at atmospheric pressure, which is a function of temperature and salinity (Warner and Weiss, 1985).

CFC-12 was used for this analysis because its atmospheric concentration continued to increase until 2001; in contrast to CFC-11 or CFC-113, which ceased to increase past 1993. Thus, CFC-12 offers a greater range for estimating ventilation ages. The time series of northern hemisphere CFC-12 atmospheric mole fraction (Walker et al., 2000) was extended through 2003 using atmospheric measurements made at Trinidad Head, California. The ventilation year was determined by comparing the pCFC-12 values to the annual mean atmospheric mole fraction of CFC-12 as a function of time, and the pCFC-12 age was found by subtracting the ventilation year from the year of collection.

We disregarded CFC-12 concentrations less than 0.02 pmol kg^{-1}, which correspond to pCFC-12 values of ~5 μatm in our data set and ventilation ages of >58 years. At this concentration, the relative measurement uncertainty is large and there is a significant fraction of CFC-free water in the water mass; both of these factors cause large errors in the pCFC-12 age (Nelson et al., 2007). The mole fraction of atmospheric CFC-12 decreased after 2002. It is not possible to assess pCFC-12 ages between 0 and 3 years, so we ascribed a zero age value to all of these samples. The precision of the CFC-12 method is often approximately the larger of 0.5% or 0.01 pmol kg^{-1} for a single laboratory, which was the case for the A20 and A22 cruises, but comparisons between the numerous WOCE data sets measured by different laboratories reveals a practical precision and accuracy of 1–3% (Fine et al., 2002). The error in the pCFC-12 age resulting from the analytical uncertainty varies as a function of the slope of CFC-12 vs. time for the atmospheric concentration curve. The minimum estimated error in ventilation age is ~0.5 years for pCFC-12 ages between 5 and 45 years. For ages between 45 and 55 years the error is ~2 years while for ages between 3 and 5 years the error is ~1 year.

CFC-12 measurement accuracy is not the only source of error in estimating ventilation age from pCFC-12 measurements. Undersaturation of CFC-12 in surface waters at time of ventilation (Fine et al., 2002) and isopycnal and diapycnal mixing of 'newer' high-CFC water with 'older' zero-CFC water (Haine and Richards, 1995; Smethie et al., 2000) introduce errors in ages estimated from CFC concentrations. To account for the wintertime CFC-12 undersaturation issue, pCFC-12 ages were determined using the best estimate of the CFC-12 saturation level in the source water region for each layer (Nelson et al., 2007). This was achieved by multiplying the atmospheric time history by the fraction of saturation and then the year of formation was determined from the pCFC value of the water samples. In some cases for near-surface water masses, the pCFC value was greater than the saturation-adjusted maximum in the atmospheric time history (Nelson et al., 2007). This discrepancy results when water becomes supersaturated, which occurs in water warmed by solar radiation and/or by mixing with warmer water. In these cases, the age was assumed to be zero.

Dispersion and mixing in the ocean typically result in pCFC ages that are younger than the true mean age (e.g., Khatiwala et al., 2001). Indeed, it would be more accurate to characterize ventilation time scales in terms of an age or transit-time distribution (Holzer and Hall, 2000; Khatiwala et al., 2001). Recent work (Waugh et al., 2004; Khatiwala et al., 2009) suggests that it may be possible to estimate these distributions from tracer data, and future work will consider this refinement. Here, we attempt to address some of the bias due to mixing by restricting our pCFC-12 age calculation to CFC-12 concentrations above 0.02 pmol kg^{-1}, thus eliminating waters where this problem was most acute. However, we recognize that waters in the older part of the age range that we use probably have a true mean age that is greater than the pCFC-12 age.

2.5. Water mass definitions

We adopted the water mass definitions of Joyce et al. (2001), based upon neutral density (γ^n) isopycnals, to investigate changes in DOC, pCFC-12 age and AOU within the meso- and bathypelagic zones of the North Atlantic. We have condensed several of the layers identified by Joyce et al. to simplify the statistical analyses (Table 2) as described in Nelson et al. (2007). Briefly, we have condensed layers 2–4 of Joyce et al. (2001) (γ^n range 25–26.4 kg m^{-3}, including the seasonal thermocline and subtropical underwater) and refer to this neutral density layer as the upper thermocline (UTCL). Subtropical mode (STMW) and lower thermocline (LTCL) waters were defined by γ^n ranges of 26.4–26.6 kg m^{-3} and 26.6–27 kg m^{-3}, respectively. For North Atlantic Deep Water (NADW), we considered Upper Labrador Sea Water (ULSW, layer 10 of Joyce et al. 2001, γ^n from 27.8 to 27.875 kg m^{-3}), Labrador Sea Water (LSW, layers 11 and 12 combined of Joyce et al. 2001, γ^n from 27.875 to 27.975 kg m^{-3}), Iceland-Scotland Overflow Water (ISOW, γ^n from 27.975 to 28.05 kg m^{-3}), and Denmark Strait Overflow Water (DSOW, γ^n from 28.05–28.14 kg m^{-3}).

2.6. Data analyses

Contouring of the data as well as computations of γ^n and AOU were performed using Ocean Data View (Schlitzer, 2004). AOU was converted to carbon equivalents (AOU-C_{eq}) using a molar ratio $-\Delta C/\Delta O2 = 0.72$ (Anderson, 1995). We recognize that this ratio may vary in nature but we chose to use this fixed ratio so that our values could be directly compared to other studies that used a similar ratio (Doval and Hansell, 2000). To reflect relationships between DOC, ventilation age, and AOU-C_{eq} within the mesopelagic and bathypelagic, we restricted all data analyses to samples collected from depths >100 m and to stations where the bottom depths were >1000 m. All statistical analyses were performed using the statistical package JMP (SAS Institute Inc., NC). All observations flagged by the analysts as "questionable" or "bad" were removed prior to analyses (7% for AOU, 1% for DOC, 0.5% for pCFC-12).

2.7. Mixing models

Changes in DOC with increasing ventilation age and AOU-C_{eq} were determined by single-end mixing model, two end-member (binary) mixing models and multiple linear regression models.

Table 2
Water mass definitions based on neutral density intervals (Joyce et al., 2001) and their relevant characteristics. Data from the three cruises were merged for this analysis. Error terms refer to standard deviation. Means are determined within each neutral density layer where data are from >100 m depth and where the bottom depth was >1000 m. '*n*' indicates number of samples. AOU-C_{eq} is calculated with AOU in carbon equivalents using a Redfield ratio -$\Delta C/\Delta O2 = 0.72$ (Anderson 1995).

Neutral Density Layer	Abbreviation	γ^n range (kg m^{-3})	Depth m (range)	theta °C	pCFC12 - age		DOC		AOU-C_{eq}	
					yr	*n*	µmol kg^{-1}	*n*	µmol kg^{-1}	*n*
Upper Thermocline	UTCL	25–26.4	170 (100–349)	20.2 ± 1.9	6 ± 6 (0–20)	365	55.4 ± 4.7	188	24.6 ± 20	418
Subtropical Mode Water	STMW	26.4–26.6	235 (100–499)	17.0 ± 1.57	13 ± 8 (0–27)	214	50.2 ± 3	120	50 ± 35	316
Lower Thermocline	LTCL	26.6–27.0	292 (102–793)	13.9 ± 1.8	19 ± 10 (0–36)	532	48.2 ± 1.8	303	73 ± 39	662
Antarctic Intermediate Water (south of 25 N°)	AAIW	27–27.8	745 (249–1486)	7.2 ± 2.3	43 ± 8 (22–58)	796	42.3 ± 1.9	498	117 ± 20	1094
Labrador Sea Water	LSW	27.80–27.975	1710 (620–4994)	4.2 ± 0.8	39 ± 10 (20–58)	1306	43.3 ± 2.1	521	53 ± 15	1432
Iceland-Scotland Overflow Water	ISOW	27.975–28.05	2333 (1331–3251)	3.1 ± 0.3	42 ± 8 (28–56)	422	42.4 ± 1.6	213	48 ± 8	566
Denmark Strait Overflow Water	DSOW	28.05–28.14	3783 (1677–5953)	2.2 ± 0.3	45 ± 7 (26–58)	961	41.6 ± 1.3	551	54 ± 8	1435
Antarctic Bottom Water	AABW	28.14–29	5019 (3931–5884)	1.4 ± 0.5	ND		40.5 ± 1.2	77	67 ± 11	179

2.7.1. Single-end member mixing model

This approach consists of a reduced major axis linear regression (model II regression) of two parameters (i.e., DOC vs. pCFC-12 age or DOC vs. AOU-C_{eq}). The slopes of the linear regression of DOC concentrations versus pCFC-12 ages and AOU-C_{eq} indicate DOC decay rates and the contribution of DOC oxidation to AOU-$C_{eq.}$, respectively. This approach does not consider the effect of horizontal mixing along isopycnal surfaces (Takahashi et al. 1985).

2.7.2. Binary mixing model

Water masses within the main thermocline of the subtropical gyre are a mixture of components formed and subducted in the eastern North Atlantic and components advected across the equator from the South Atlantic (Schmitz and Richardson, 1991; Schmitz, 1996; Hansell et al., 2004). Hence, the correction for isopycnal mixing and advection may be important for assessment of the biogeochemical processes regulating DOC concentrations in the meso- and bathypelagic.

The contribution of mixing can be assessed with a two-component potential temperature and salinity calculation within neutral density layers (γ^n range of 25–27 kg m^{-3}), in which boundaries of the data cloud represent the southern (SC) and northern components (NC), respectively (see Hansell et al., 2004). Characterizations of NC and SC for the UTCL, STMW and LTCL neutral-density layers were performed using data from the CLIVAR A16N line.

Potential temperature (θ) is distributed linearly against γ^n within the main thermocline of the subtropical North Atlantic (see Hansell et al., 2004). Within UTCL, STMW and LTCL, the data cloud of θ *vs* γ^n were constrained by clear boundaries of data that correspond to the coldest and warmest waters and represent the locally purest forms of SC and NC, respectively. Mixing of these end members largely occurs along isopycnal surfaces, so water mass temperatures intermediate to NC and SC indicate the degree of mixing between those end members. The fractions of the northern (F_n) and southern (F_s) end-members can be determined once θ of the NC and the SC are characterized, following Takahashi et al. (1985):

$$F_s = (\theta^o_n - \theta_{obs})/(\theta^o_n - \theta^o_s) \quad (1)$$

and

$$F_n = 1 - F_s \quad (2)$$

where θ^o_n *and* θ^o_s are the potential temperatures of the NC and SC, respectively, and θ_{obs} is the observed potential temperature. Linear regressions of DOC, AOU-C_{eq} and pCFC-12 age versus γ^n, with data from regions characterized as essentially pure NC and SC water, were used to assign values for these variables at specific neutral densities within each end member. Table 3 presents the latitudinal range and means of the derived values for the end members of UTCL, STMW and LTCL. The preformed concentration or age for each sample, C°, was thus determined by

$$C^\circ = F_n C^\circ_n + F_s C^\circ_s \quad (3)$$

where C°_n and C°_s are the preformed quantities in the northern and southern end-members, respectively (Takahashi et al., 1985). The change in a measured quantity due to processes other than mixing (*C) was determined by

$$^*C = C_{obs} - C^\circ \quad (4)$$

where C_{obs} is the observed quantity of DOC, pCFC-12 age or AOU-C_{eq}

We were unable to accurately determine the end-member contribution for water masses below the main thermocline due to the complicating influences of a third end-member, the

Table 3
Latitudinal range and mean water mass characteristics for the northern and southern components of the UTCL, STMW and LTCL waters along the A16 line. Error represents standard deviation of the mean.

	Northern Component	Southern Component
UTCL	γ^n *25–26.4* kg m^{-3}	
Latitude	21.5°N–26°N	5°S–2.6°N
θ (°C)	22.17 ± 1.8	17.8 ± 2.1
Salinity	37.40 ± 0.2	35.8 ± 0.2
DOC (μmol kg^{-1})	66 ± 5.6	57 ± 4.6
pCFC-12 age (yrs.)	0	15 ± 6
AOU-C_{eq} (μmol kg^{-1})	1.3 ± 11	72 ± 26
STMW	γ^n *26.4–26.6* kg m^{-3}	
Latitude	25°N–32.5°N	3°S–4.5°N
θ (°C)	18 ± 0.5	14.4 ± 0.5
Salinity	36.6 ± 0.1	35.5 ± 0.1
DOC (μmol kg^{-1})	54.5 ± 4	49.3 ± 2.7
pCFC-12 age (yrs.)	0	21.6 ± 2
AOU-C_{eq} (μmol kg^{-1})	14 ± 11	98 ± 21
LTCL	γ^n *26.6–27* kg m^{-3}	
Latitude	28°N–37.5°N	5°S–5°N
θ (°C)	15.2 ± 1.1	12.0 ± 1.2
Salinity	36.1 ± 0.2	35.16 ± 0.1
DOC (μmol kg^{-1})	50.8 ± 3	46.5 ± 1.8
pCFC-12 age (yrs.)	1.3 ± 4.2	26.7 ± 3.3
AOU-C_{eq} (μmol kg^{-1})	25 ± 9	114 ± 18

Mediterranean Overflow Water. Thus, a binary mixing model correction could not be performed for those water masses.

2.7.3. Multiple linear regression

A multiple linear regression model can be used in cases of up to three end-member mixing when the chemical properties of the end-members are unknown (Schneider et al., 2005). To estimate DOC decay rates the following multiple linear regression was performed:

$$DOC = \alpha_1 + \alpha_2\theta + \alpha_3 S + \alpha_4 pCFC12age \quad (5)$$

Here the linear regression coefficients α_1, α_2, and α_3 quantify the linear mixing of three end-member characteristics in potential temperature (θ), salinity (S) and pCFC-12 age under the assumption of mass conservation. The coefficient α_4 is thus the contribution of DOC decay rate for a neutral density layer independent of mixing. A similar expression can be written to assess the contribution of DOC oxidation to AOU-C_{eq}:

$$DOC = b_1 + b_2 q + b_3 S + b_4 AOUC_{eq} \quad (6)$$

where β_1 , β_2, and β_3 carry the three end-member characteristics of θ and S and β_4 is the contribution of DOC oxidation to AOU-C_{eq} independent of mixing (see Schneider et al., 2005 for further details of this approach).

3. Results and discussion

3.1. Meridional trends in mean DOC concentrations within the euphotic, mesopelagic and bathypelagic zones

Characteristics of North Atlantic water masses considered here are presented in Table 2. In general, water masses of higher density had elevated pCFC-12 ages and AOU-C_{eq}, and lower DOC concentrations. Mean DOC concentrations demonstrate systematic meridional trends within depth horizons characteristic of the epipelagic zone (0–100 m), mesopelagic zone (100–1000 m) and bathypelagic zone (1000–3000 m) (Fig. 2). The mean euphotic zone DOC concentration maxima were observed in the highly

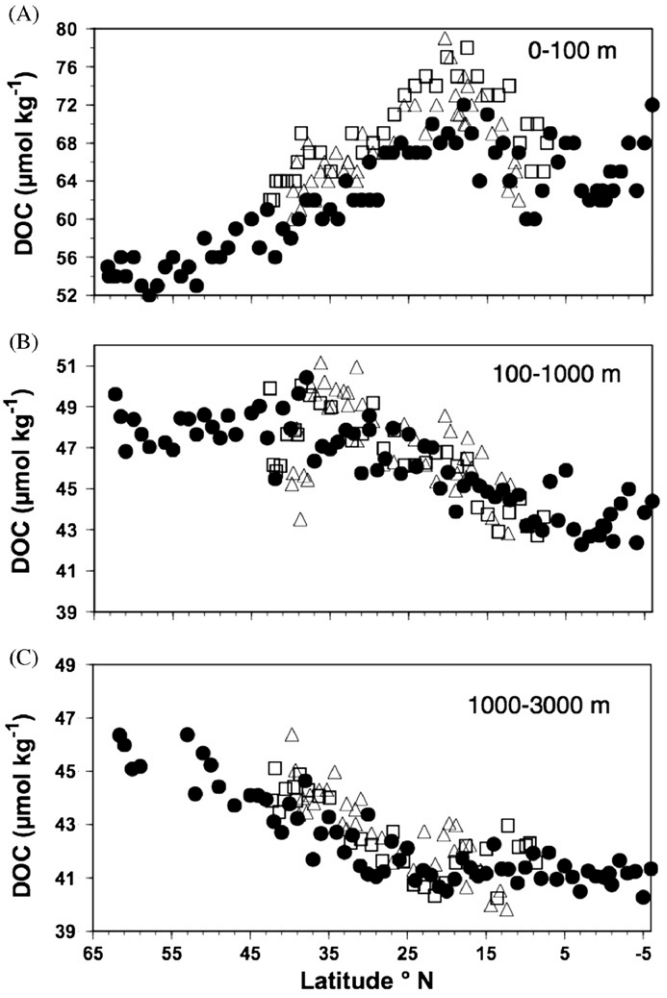

Fig. 2. Meridional distributions of mean DOC concentrations for the euphotic zone (0–100 m) (A), the mesopelagic zone (100–1000 m) (B), and the bathypelagic zone (1000–3000 m) (C). Mean DOC concentrations were determined by integrating DOC stocks within each depth horizon for each hydrostation and normalizing to the depth of each depth horizon. Filled circles, open triangles, and open squares are DOC values from A16, A22, and A20, respectively. Note scales of the y-axes differ between panels.

stratified regions of the subtropical gyre between 15–20°N (Fig. 2A). To the south, epipelagic DOC concentrations decreased in part due to the equatorial upwelling of low DOC subsurface water and subsequent poleward transport via wind driven circulation. To the north, ventilation of deeper waters intensified; thus, low-DOC water was entrained from depth to the surface, diluting the near-surface DOC concentrations (Fig. 2A).

As a consequence of convective mixing and isopycnal ventilation at high latitudes, the surface accumulated DOC, which had resisted rapid microbial remineralization, was exported from the surface layer into the mesopelagic and bathypelagic zones (Fig. 2B,C) poleward of 35°N. DOC concentration gradients were generated within mesopelagic and bathypelagic zones due to a combination of DOC remineralization and mixing with low-DOC waters flowing northward from the South Atlantic (Hansell and Carlson, 1998, Amon et al. 2003). The lack of a DOC gradient north of 35°N in the mesopelagic depth horizon (Fig. 2B) is indicative of recent ventilation and water column renewal in which seasonal export of DOC into the mesopelagic occurred in the northern reaches of the transect. The sustained gradient in the bathypelagic realm indicates that export of DOC into this depth horizon was most pronounced at latitudes north of 50°N.

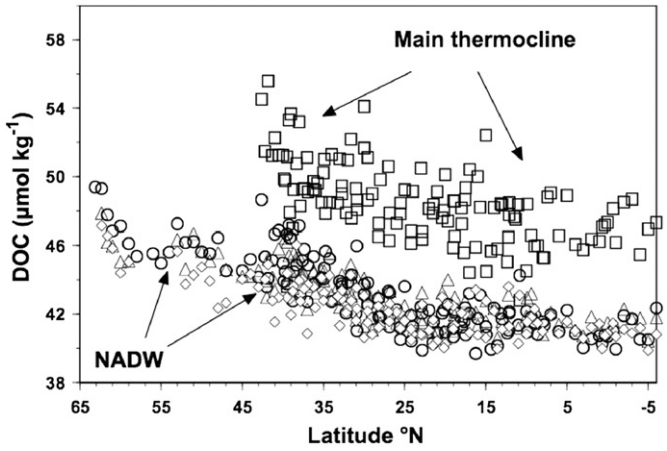

Fig. 3. Meridional distribution of mean DOC concentrations within water masses of the main thermocline and NADW as determined in Fig. 2 except integrated values were normalized to thickness of the neutral density layer at each hydrostation. The open squares represent mean DOC concentrations in the STMW and LTCL water masses. The open circles, open triangles, and open diamonds represent the LSW, ISOW and DSOW of the NADW, respectively. Water mass definitions are given in Table 2.

3.2. DOC export

DOC export via convective overturn can be an important component of the biological pump (Copin-Montégut and Avril, 1993; Carlson et al., 1994; Ducklow et al., 1995; Hansell and Carlson, 2001a; Kähler and Koeve, 2001; Hopkinson and Vallino, 2005). Basin scale estimates of DOC export can be calculated as the product of the mean DOC-concentration decrease (ΔDOC) within a given water mass (Fig. 3) and the ventilation rate of that water mass (Hansell and Carlson, 1998; Hansell et al., 2002; Amon et al., 2003). To evaluate the ΔDOC within each water mass, we plotted mean DOC versus latitude (Fig. 3). Values of ΔDOC in the main thermocline (γ^n=26.4–27 kg m^{-3}) and in NADW (comprising LSW, ISOW, DSOW) were determined from the linear regression of DOC versus latitude between 43–9°N and 63–19°N, respectively. There was no significant change in DOC to the south of 9°N or 19°N in the main thermocline or NADW, respectively, thus those stations were removed from the regression analyses to determine ΔDOC. ΔDOC in the main thermocline and the NADW were 6 ± 1 and 6 ± 0.6 mmol C m^{-3}, respectively (Table 4). ΔDOC together with ventilation rate estimates of ~16 Sv (Sv=10^6 m^3 s^{-1}) for the subtropical and subpolar thermocline (Haine et al., 2003) and 17.2 Sv for NADW (Smethie and Fine, 2001) indicates net DOC export of $\sim6.4\times10^{12}$ mol C yr^{-1} (0.077 Pg C yr^{-1}) out of the epipelagic zone into the mesopelagic and bathypelagic zones. An additional 0.004 Pg C yr^{-1} of DOC export has been reported for the Greenland Sea (Amon et al., 2003), north of our study, bringing estimates of DOC export into the interior of the North Atlantic to ~0.081 Pg C yr^{-1}.

The calculated export rate is most sensitive to the water mass ventilation rates chosen as the ΔDOC estimates appear to be well constrained. We chose conservative (low) estimates of water-mass ventilation of the main thermocline and NADW. In fact, estimates of ventilation rates vary significantly (i.e., 12–88 Sv ; see Hansell et al. 2007 for a discussion of published estimates of main thermocline ventilation within the subtropical North Atlantic). Using those ventilation rates to estimate DOC export would also scale accordingly.

DOC exported into the North Atlantic contributes to the total export of carbon via the biological pump. Estimates of total export production based on changes in oxygen inventories in the North Atlantic during the spring- summer period (north of 15°N) range from 0.4–0.6 Pg C (Louanchi and Najjar, 2001). Inverse modeling within the latitudinal range of 0°–70°N yields an export of ~0.86 Pg C yr^{-1} (Schlitzer, 2000). Export production calculated from seasonal changes in dissolved inorganic carbon was 0.8 Pg C yr^{-1} between 40°N–70°N (Lee, 2001). Allowing for discrepancies in the time and space scales used to calculate these various export rates, DOC export represents ~9 to 20% of total export production within the North Atlantic. This contribution falls within the range of other studies in the North Atlantic. Sohrin and Sempere (2005) found that DOC export via convective overturn contributed, on average, <10% (range 0–32%) of new production in the northeast Atlantic. Shallow DOC export at the Bermuda Atlantic Times-series Study site in the Sargasso Sea ranged from 15 to 41% of export production (Hansell and Carlson, 2001a), and modeling efforts have estimated DOC export to be ~37% of new production in the Labrador Sea (Tian et al., 2004).

Table 4
Ventilation rates, changes in mean DOC concentrations (ΔDOC) and DOC export rates within the main thermocline and NADW. Ventilation rates for the main thermocline and NADW were taken from Haine et al. (2003) and Smethie et al. (2001), respectively. Water mass definitions are given in Table 2.

Water Mass	Ventilation Rate Sv (1×10^6 m^3 s^{-1})	ΔDOC* mmol m^{-3}	DOC Export Pg C yr^{-1}
Main Thermocline density (26.35–27.13)	16	6 ± 1	0.037
NADW Including LSW, ISOW and DSOW	17.2	6 ± 0.6	0.04
Summed DOC export rate			0.077

* Change in mean DOC concentration as determined by Model I regression of all mean DOC concentrations versus latitude using depth-normalized DOC means within the main thermocline (43°N–9°N) and NADW (65°N–19°N).

3.3. Vertical and horizontal variability of DOC in the north atlantic interior

The present observations provide unprecedented detail of the spatial distribution of DOC within North Atlantic along lines A16 (Fig. 4A), A20 (Fig. 5A) and A22 (Fig. 6A). North of 50°N (Fig. 4A), DOC concentrations as high as 47 µmol C kg^{-1} reach depths >2000 m due to NADW formation. Further south, the DOC concentrations declined to <42 µmol kg^{-1}, a concentration found throughout much of the bathypelagic zone.

Some of the low DOC concentrations found in the eastern Atlantic and central subtropical gyre were due to the presence of low DOC water introduced from the South Atlantic. The lowest DOC concentrations (~38 µmol kg^{-1}) observed were located in Antarctic Bottom Water (AABW), located south of the equator on A16N (Fig. 4A). Northward transport of that water introduces low DOC into the deep North Atlantic. Evidence for its influence is seen in a bolus of low DOC water (39–42 µmol kg^{-1}) observed at >2000 m between 12–27°N on A20 (Fig. 5A) and 20–27°S on A22 (Fig. 6A). This bolus was flanked to the north and south by water with higher DOC concentrations. DOC on the 27.9 kg m^{-3} neutral density surface illustrates the nature of this observation (Fig. 1). DOC-enriched NADW has westward flow across the northern end of A20 and eastern flow across the southern end, thus creating the pattern observed at depth. At shallower depths (500–1200 m) a tongue of low DOC water (i.e., 39–42 µmol kg^{-1}) extending from South America to 30°N along 52°W demonstrates the influence of Antarctic Intermediate Water (AAIW; Fig. 5A). The high spatial variability and low DOC concentrations observed in the deep North Atlantic were surprising given that values <39 µmol kg^{-1}

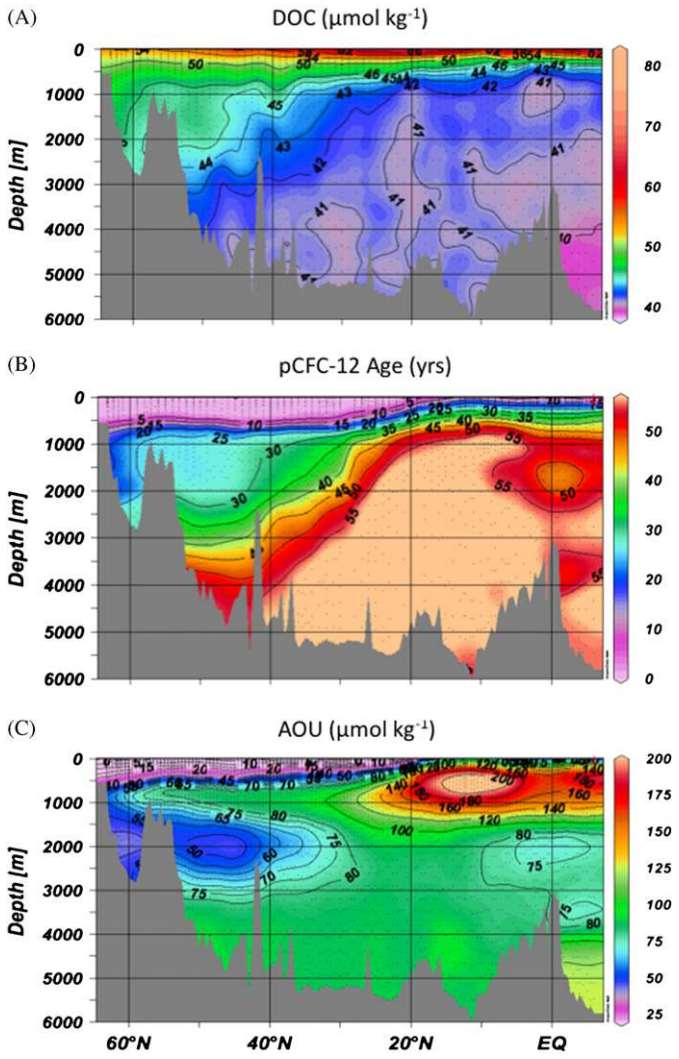

Fig. 4. Contours of A) DOC (μmol kg^{-1}), B) pCFC-12 ages (yrs), and C) AOU (μmol kg^{-1}) for the A16N CLIVAR line (longitude 20°–29°W).

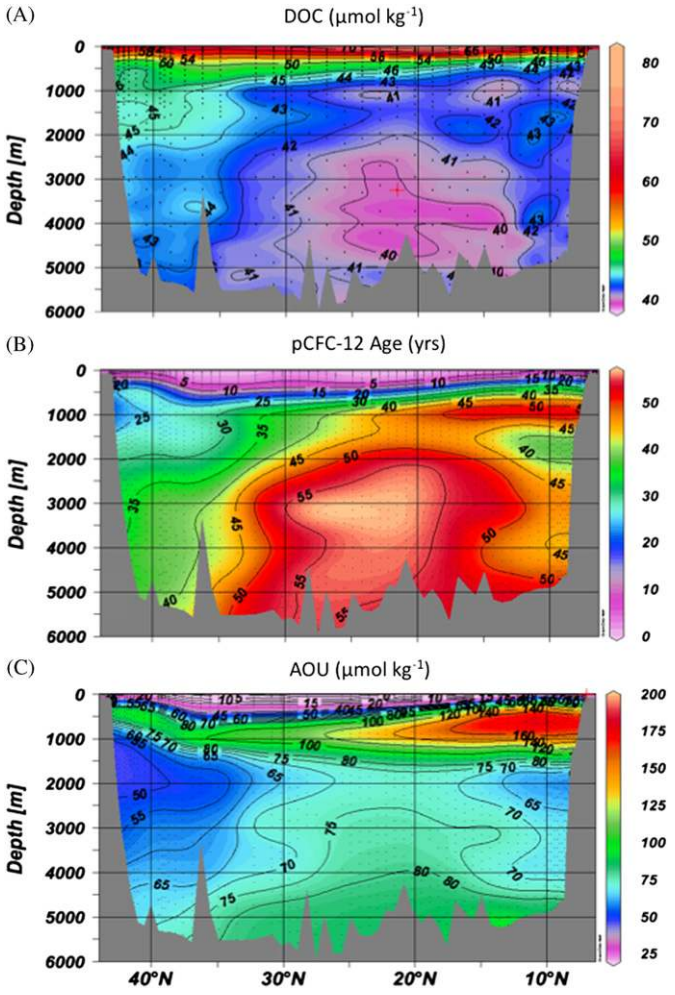

Fig. 5. Contours of (A) DOC (μmol kg^{-1}), (B) CFC-12 ages (yrs), and C) AOU (μmol kg^{-1}) for the A20 CLIVAR line (longitude 52°W).

had previously only been reported in the deep equatorial Pacific and the North Pacific, where the oldest deep waters are located and low DOC is anticipated (Druffel et al., 1992; Hansell and Carlson, 1998).

Previous work in the North Atlantic demonstrated little temporal or vertical variability of DOC at >1500 m for any given site (Hansell and Carlson, 2001a; Kähler and Koeve, 2001; Amon et al., 2003; Sohrin and Sempere, 2005). However, when comparing DOC concentrations collected from a great latitudinal range, gradients have been observed. For example, studies of deep-water masses in the Nordic Sea show DOC concentrations of $\sim$49 μmol kg^{-1} (Amon et al. 2003) compared to $\sim$43 μmol kg^{-1} between 32–44°N (Hansell and Carlson 2001, Sohrin and Sempéré 2005). Within a single study a gradient of 4 μmol kg^{-1} DOC had been observed in deep waters between 75°N and 32°N (Hansell and Carlson, 1998). However, we are not aware of any study that has demonstrated the degree of deep DOC variability observed here. This variability has gone undetected due to the paucity of spatially distributed observations from the ocean interior.

3.4. Estimates of DOC decay rates

One of the challenges in marine organic matter biogeochemistry is determining decay rates for DOC deep within the various ocean basins (Williams, 2000, Arístegui et al., 2005). Historically the bulk of deep DOC has been thought to be composed of refractory DOC that is resistant to short term microbial remineralization (Barber, 1968). Hansell and Carlson (1998) examined the change of DOC in the deep waters along the deep-ocean conveyor and suggested that there was a portion of the deep DOC pool that was recalcitrant but was slowly remineralized over time scales of decades to centuries. It is not possible to assess decay rates of this recalcitrant DOC pool with short-term microbial incubation experiments due to extremely slow rates for this process. However, spatial DOC gradients coupled with pCFC-12 ages can be used to constrain the DOC decay rates of a portion of the exported DOC within a given water mass. All pairwise DOC and pCFC-12 age data assessed here were retrieved from water masses within the main thermocline and NADW, taking the slopes of model II linear regression as the DOC decay rates. Rates derived from single end-member model II regressions ranged from 0.18 to 0.94 μmol kg^{-1} yr^{-1}, with the lowest rates occurring in the high density water masses (Table 5).

A binary mixing model was used to account for the effects of two end-member mixing within the UTCL, STMW, and LTCL (Table 5). For these water masses, slopes of model II (major reduced axis) linear regression were calculated for all pairwise *DOC and *pCFC-12 age data observations (where the star variables are the changes in that variable due to processes other

than mixing). The mixing-corrected DOC decay rates were within ~30% of rates derived using the single-end-member mixing model for the main thermocline water masses. As described previously, the influence of Mediterranean Overflow Water in the eastern North Atlantic precluded the binary mixing model correction of deeper water masses. DOC removal rates derived from the multiple linear regression approach, though, can be applied in cases where there are up to three end-members

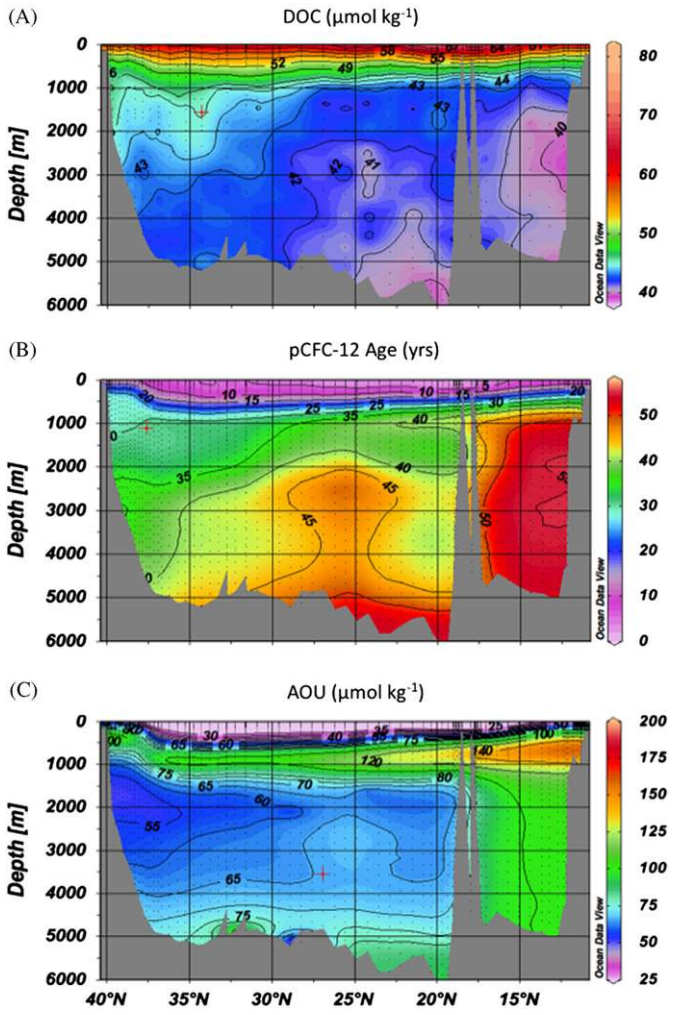

Fig. 6. Contours of (A) DOC (μmol kg^{-1}), (B) CFC-12 ages (yrs), and (C) AOU (μmol kg^{-1}) for the A22 CLIVAR line (longitude 66°W).

(Schneider et al., 2005). Rates derived with this approach were systematically lower for each water mass (Table 5) compared to the other model derivations. However the multiple linear regression decay rates were within ~35% of estimates derived from the simple linear regression model for the LTCL, LSW, ISOW and DSOW water masses. The differences between rates derived using multiple linear regression and the other models was most pronounced in the UTCL (γ^n 25–26.4 kg m^{-3}) and STMW (γ^n 26.4–26.6 kg m^{-3}) (Table 5).

There are several differences between the various models that may lead to discrepancies between the derived DOC decay rates. The simple linear regression using model II regression infers a removal rate within a neutral density and assumes that changes within an isopycnal layer arise exclusively from processes other than mixing. The estimates based on this simple linear regression can yield bias in the gradients of the variable induced by variable end-member contributions within a neutral density layer (Takahashi et al., 1985). Two-component mixing models (i.e. northern and southern; described above) have been used to examine distributions of nutrient tracers along isopycnal surfaces independent of mixing (Gruber and Sarmiento, 1997; Hansell et al., 2004; Takahashi et al., 1985). However, this approach is highly sensitive to changes in the assumptions or error associated with these prescribed values (Schneider et al., 2005). The multiple linear regression approach determines the mixing of up to three end-members without the need to define the end-members. However, in reality the composition of each point in a water mass is composed of multiple sources, thus, what this approach assumes to be an end-member is already a mixed product of several sources with different remineralization history (Schneider et al., 2005). Previous work evaluating nutrient regeneration found that the multiple linear regression approach showed very good agreement with a 3-D ocean circulation of the oceanic carbon cycle for dense lower thermocline and NADW water masses (Schneider et al., 2005). However, it is not clear how well this approach works in tracking nutrient tracers in lighter and shallower water masses such as the UTCL and STMW.

3.4.1. *Comparison with previously published estimates of DOC decay*

The bulk DOM pool represents various pools of biological lability that can be conceptually partitioned into the labile, semi labile, and refractory pools (Carlson, 2002). The decay rates derived from the various water masses ranged from 0.13 to 0.93 μmol kg^{-1} yr^{-1} (Table 5) and are 3–4 orders of magnitude smaller than those that are typically representative of labile DOM measured in short-term microbial remineralization experiments (i.e., ~1 μmol kg^{-1} d^{-1}; Zweifel et al., 1993; Carlson and Ducklow, 1996; Cherrier et al., 1996). These DOC decay rates are

Table 5
DOC removal rates estimated from Model II reduced major axis regression statistics for single end-member mixing (DOC vs. pCFC-12 age), binary mixing (*DOC vs. *pCFC-12 age), and a multiple linear regression model by water mass as defined in Table 2. Standard errors are given. All values are significant at the 95% confidence interval; nd refers to not determined. 'n' is the number of data pairs used for each model.

Water mass	DOC Removal Rate					
	Single end-member mixing			Binary Mixing[a]		Multiple Linear regression
	(μmol kg^{-1} y^{-1})	n	r^2	(μmol kg^{-1} y^{-1})	r^2	(μmol kg^{-1} y^{-1})
UTCL	0.93 ± 0.06	167	0.33	0.79 ± 0.05	0.3	0.25 ± 0.06
STMW	0.33 ± 0.03	105	0.27	0.45 ± 0.04	0.18	0.17 ± 0.04
LTCL	0.25 ± 0.01	311	0.38	0.30 ± 0.01	0.38	0.18 ± 0.01
LSW	0.20 ± 0.01	436	0.69	nd		0.17 ± 0.01
ISOW	0.18 ± 0.01	141	0.58	nd		0.14 ± 0.01
DSOW	0.20 ± 0.01	278	0.53	nd		0.13 ± 0.01

[a] Corrected for binary mixing and represents change in variable due to processes other than mixing.

also significantly lower than those estimated from time-series monitoring of DOC variability in the mesopelagic zone (i.e. 2–10 μmol kg^{-1} yr^{-1}; Copin-Montégut and Avril, 1993; Hansell and Carlson, 2001a; Sohrin and Sempere, 2005), but are comparable to those derived from vertical DOC gradients and ventilation rates in the Greenland Gyre of 1–2.5 μmol kg^{-1} yr^{-1} at ~1500 m, and 0.05 μmol kg^{-1} yr^{-1} at depths > 1500 m (Amon et al., 2003). These results suggest that the slow decay rates observed in the interior of the North Atlantic characterize a portion of exported DOC that is more recalcitrant than portions of the semi-labile DOC pool that turn over on time scales of days to months, but that is more labile than the refractory DOC that is removed on time scales of centuries to millennia. We term this pool semi-refractory DOC.

The values of ΔDOC reported in Table 4 represent the portion of exported DOC that is removed within the North Atlantic. Dividing ΔDOC by the DOC decay rates (Table 5) gives mean ΔDOC turnover times of 6 to 33 y within the main thermocline and ~30–46 y for the NADW. These turnover times are orders of magnitude faster than the millennial scale turnover times predicted from ^{14}C age of the deep bulk DOC pool (Druffel et al., 1989; Bauer et al., 1992). The mean ^{14}C age of DOC in the north Atlantic is 3970 yrs., indicating that a significant fraction of the deep DOC turns over on time scales of millennia. However, DOC fractions of varying lability and ^{14}C enrichment comprise the bulk DO^{14}C signature. Bauer (2002) shows a DOC age difference of 1600 years between the Sargasso Sea and the Southern Ocean, suggesting that a small fraction of the deep DOC pool (enriched in ^{14}C) might be utilized during deep-ocean transect through the Atlantic.

The turnover rates of the ΔDOC of the mesopelagic and bathypelagic zones indicate that the quality of the DOC in these depth horizons is relatively more bioavailable compared to the majority of the deep refractory DOC observed in the south Atlantic and Pacific Ocean (Hansell et al., 2009). The trend of elevated turnover of deep DOC has also been reported by Santinelli et al. (2010) for waters of the Mediterranean Sea. Chemical composition of DOC in the deep Mediterranean Sea indicates that the exported DOC is relatively bioavailable (Meador et al., 2010).

At first glance the low decay rates of exported DOC (i.e., 0.13–0.93 μmol kg^{-1} yr^{-1}) in the North Atlantic appear to be comparable to recent reports of prokaryotic production (Herndl et al. 2005). For example, heterotrophic prokaryotic production rates of 1.1 to 2.1 nmol C L^{-1} d^{-1} based on short-term (hours) ^{3}H - Leucine incubations have been reported for waters in the deep North Atlantic (Herndl et al., 2005; Reinthaler et al., 2006). However, the carbon demand associated with the measured heterotrophic production is a function of how efficiently the organisms utilize the organic matter (i.e. heterotrophic prokaryotic carbon demand = heterotrophic prokaryotic production / growth efficiency). Prokaryotic growth efficiencies have been estimated at 2% for the same deep waters (Reinthaler et al., 2006) indicating an annual prokaryotic carbon demand of ~20–38 μmol C L^{-1} y^{-1}. Combined these data suggest that heterotrophic microbes in the North Atlantic dark ocean are metabolically active (Herndl et al., 2005; Teira et al., 2006) and sustain relatively high carbon demands (Reinthaler et al., 2006). The derived annual carbon demand is several orders of magnitude greater than the DOC decay rate estimated or deep DOC gradients observed in this study. The carbon demand of the deep microbial consortia is also greater than the flux of POC into the ocean interior (Reinthaler et al., 2010). This uncoupling between prokaryotic carbon demand, POC flux and observed DOC removal point to problems in balancing the carbon budget in the mesopelagic and bathypelagic zone (Steinberg et al., 2008; Arístegui et al., 2009; Burd et al., 2010; Robinson et al., 2010). Some of this discrepancy may be due to inadequacies of methods, poorly constrained conversion factors and growth efficiencies (Burd et al., 2010), or it may indicate alternative sources of DOC that do not accumulate but fuel the active microbial consortia. Recently, chemoautotrophy in the ocean's interior has been recognized as a potentially important source of "new" carbon to fuel the mesopelagic and bathypelagic microbial carbon demand (Herndl et al., 2005; Ingalls et al., 2006; Hansman et al., 2009; Reinthaler et al., 2010),which may help account for some of the discrepancy.

3.4.2. Trends in DOC decay rates

The DOC decay rates derived from the single end-member and the multiple linear regression models both show a decreasing trend with increasing density layer and with decreasing temperature (Tables 2 and 5). These data suggest a potential temperature control on heterotrophic microbial activity and subsequent remineralization of organic substrates (Shiah and Ducklow, 1994; Bendtsen et al., 2002). We investigated the apparent temperature dependence of DOC decay in the North Atlantic interior to determine if it was indicative of an Arrhenius function. If DOC decay was a sole function of temperature one would expect the relationship between the natural logarithm of the DOC decay rate vs. the reciprocal of the absolute temperature in Kelvin to be a straight line (Fig. 7). The criterion of a linear fit was not met by either model, indicating that temperature was not the sole control of DOC decay. A complex mixture of compounds with varying reactivity would preclude a simple first order relationship with temperature; thus quality and subsequent diagenetic transformation of exported DOC must also be considered as important factors controlling the decay of DOC in the ocean interior.

Previous work has demonstrated vertical trends in remineralization of organic matter with preferential remineralization of protein and phosphorus compounds at shallower depths followed by preferential carbohydrate removal at greater depths (Álvarez-Salgado et al., 2006; Castro et al., 2006). Diagenetic alteration of bulk DOC also increases with depth and time (Skoog and Benner, 1997; Amon et al., 2001; Benner, 2002; Goldberg et al., 2009, Meador et al., 2010). A trend of decreasing decay rate with decreasing mean DOC concentration is consistent with the hypothesis that as DOC is subjected to microbial utilization, the

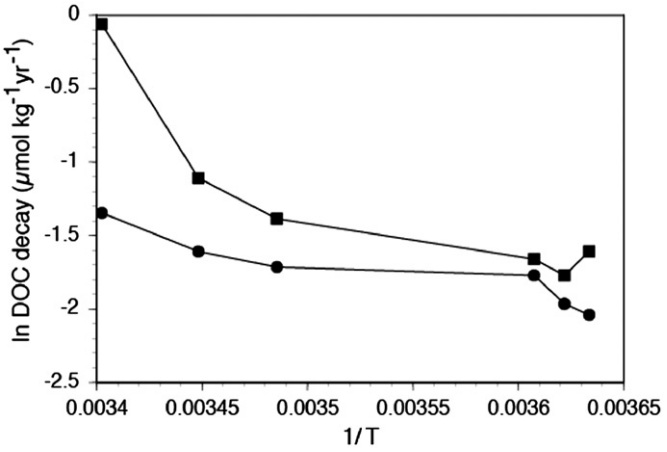

Fig. 7. Assessment of the Arrhenius function of DOC decay versus temperature where ln k (DOC decay rate) is regressed against 1/T (temperature in degrees Kelvin). Departure from a straight line indicates that the assumptions of an Arrhenius function are not met. Squares and circles represent ln DOC decay values derived using single end-member and multiple linear regression models, respectively.

most labile compounds are utilized first, leaving behind recalcitrant materials that are degraded more slowly (Cowie and Hedges 1994; Amon et al., 2001; Benner, 2002).

3.4.3. Further consideration of decay rate calculations

The meridional circulation features for the interior of the North Atlantic are reflected by the distribution of pCFC-12 ages (Smethie et al., 2000; Smethie and Fine, 2001) (e.g., Figs. 4B and 5B). Details of the age distribution within each water mass of the North Atlantic are discussed in detail elsewhere (e.g., Doney et al., 1997; Smethie et al., 2000). Accurate DOC decay rates are reliant on accurate estimates of the time for water to travel from its region of formation to the site of sampling, i.e. the water-mass age. A parcel of water comprises several components with unique ages, and it is the mean age of these components that is most appropriate for calculating a variable's rate of change (Smethie et al., 2000; Smethie and Fine, 2001; Nelson et al., 2007). The use of pCFC-12 to approximate mean water age is most accurate when all of the components of a water parcel were formed after the time when CFC-12 begin entering the ocean (Smethie et al., 2000; Smethie and Fine, 2001; Nelson et al., 2007). This condition is met for most of the thermocline and STMW of the North Atlantic, however denser water masses will include components that were formed prior to CFC-12 input. As discussed previously, the pCFC-12 age in this case will be younger than the mean age. Thus, the DOC decay rates calculated for LSW, ISOW and DSOW should be considered the upper bound of DOC decay rates. New approaches examining three-dimensional transport are being developed to assess the transit time distribution of tracers and mean water ages (Khatiwala, 2007). Application of these approaches is beyond the scope of this study but may improve ventilation age estimates in future analyses.

Understanding of the bacterioplankton community structure and function is also important for assessing DOC decay rates and microbial remineralization (Carlson et al., 2004; Arístegui et al., 2009). Heterotrophic bacterioplankton are recognized as the dominant consumers of DOM in the ocean (Azam and Hodson, 1977; Williams, 1981; Azam et al., 1983). However, removal of DOC attributed to abiotic processes cannot be ruled out. UV photolysis in the surface layer can oxidize refractory organic matter (Mopper and Kieber, 2002), transforming "refractory" DOC to a biologically available form (Benner and Biddanda, 1998). This process is constrained though to the upper euphotic zone and thus not directly responsible for the decay observed at mesopelagic and bathypelagic depths. Other abiotic DOC removal processes, such as sorption to particulate surfaces, may be important as a deep-ocean DOC sink (Druffel and Williams, 1990). Biopolymers imbedded in seawater, such as gels and transparent exopolymers (Passow and Alldredge, 1994; Wells, 1998; Aluwihare et al., 1997), move organic molecules up the particle size spectrum to sizes capable of sedimentation from the water column (Verdugo et al., 2004; Engel et al. 2004; Verdugo and Santschi, 2010). Sorption of old refractory DOC onto particles suspended in the deep ocean has been proposed to explain depleted ^{14}C signatures of those particles (Druffel et al., 1996, 1998).

3.5. DOC and AOU

Establishing the contribution of DOC to export can be examined by normalizing the changes in DOC concentrations to changes in AOU-C_{eq}. AOU derives from the mineralization of sinking biogenic particles and of subducted DOC and so reflects the total oxidation of biogenic carbon along specified surfaces (Ogura 1970). The contribution of DOC oxidation to oxygen consumption within the various water masses was determined after converting AOU to carbon equivalents. As described above, single end-member mixing, binary mixing, and multiple linear regression models (as described above for decay rate calculations) were used to derive the percent contribution of DOC oxidation to AOU-C_{eq} (Table 6) (analysis restricted to AOU-$C_{eq} > 0$ μmol kg^{-1}). The results of the various approaches indicate that 5 to 28% of the AOU-C_{eq} could be assigned to DOC oxidation while mineralization of sinking biogenic particles drove the balance of the AOU.

The greatest variability in the % contribution of DOC oxidation to AOU derived by the various model approaches was observed in the UTCL and STMW (Table 6). At the high end the elevated ratios of DOC to AOU-C_{eq} (~20–30%) derived from the single end-member (UTCL) and binary mixing model (UTCL and STMW) are consistent with previous reports for the upper portion of the thermocline of other ocean sites in the Pacific and Indian Oceans and the Gulf of Mexico (Ogura, 1970; Druffel et al., 1992; Guo et al., 1994; Doval and Hansell, 2000; Arístegui et al., 2002, 2003). However, on the low end the estimates from the single end-member mixing (STMW) and multiple linear regression model (UTCL and STMW) (5–9%) were significantly lower than previously published results. In the UTCL it is not clear whether the multiple linear regression model was appropriate for this water mass or if the previous studies using model II linear regression models properly accounted for isopycnal mixing. Nonetheless the significant variability between the model estimates in the shallower-water masses remains unclear and requires further study.

Estimates derived from the single end-member mixing and multiple linear regression models were comparable for all water

Table 6
The % contribution of DOC oxidation to AOU C_{eq} estimated from Model II reduced major axis regression of single end-member mixing (DOC vs AOU-C_{eq}), binary mixing (*DOC vs. *AOU-C_{eq}) and multiple linear regression model by water masses defined in Table 2. Standard errors are given. All values are significant at the 95% confidence interval; nd refers to not determined. '*n*' is the number of data pairs used for each model.

Water mass	Contribution of DOC Oxidation to AOU-C_{eq}					
	Single end-member mixing			Binary Mixing		Multiple Linear regression
	%	*n*	r^2	%	r^2	%
UTCL	28 ± 2	161	0.24	17 ± 1	0.26	9 ± 1
STMW	9 ± 1	109	0.17	20 ± 2	0.07	5 ± 2
LTCL	7 ± 1	332	0.34	10 ± 1	0.31	5 ± 1
LSW	14 ± 1	464	0.52	nd		12 ± 1
ISOW	19 ± 1	192	0.55	nd		14 ± 1
DSOW	16 ± 1	487	0.35	nd		9 ± 0.01

* Corrected for binary mixing and represents change in variable due to processes other than mixing.

masses denser than the UTCL, and demonstrated a similar trend in which the % DOC to AOU-C_{eq} reached a minimum in the STMW and LTCL (mean $7 \pm 2\%$) and increased in the water masses of the NADW (mean $14 \pm 3\%$) (Table 6). Previous studies have demonstrated that DOC oxidation explained $<10\%$ of AOU-C_{eq} in the deep Pacific and Indian Oceans (Menzel, 1964; Ogura, 1970; Peltzer and Hayward, 1996; Doval and Hansell, 2000; Arístegui et al., 2002, 2003); however, our results indicate that DOC export and subsequent remineralization could explain $\sim$9–19% of the AOU-C_{eq} in NADW. We attribute the greater DOC:AOU C_{eq} in the interior of the North Atlantic to the export of water with higher concentrations and, perhaps, more bioavailable DOC during NADW formation than in the other water masses considered. High contributions of DOC oxidation to AOU in deep waters have been observed elsewhere. Meador et al. (2010) reported that DOC oxidation accounted for 32% of AOU in the eastern Mediterranean Sea. Santinelli et al. (2010) found that as much as 92% of AOU in the deep Adriatic Sea was due to export and subsequent remineralization of high quality DOC. While not as great as in the Mediterranean Sea, the change in AOU-C_{eq} driven by the oxidation of DOC (5–29%) in the North Atlantic is comparable to the estimates of DOC export to total export production (9–19%) described above.

Although the importance of DOC export to the biological pump and recycling of elements in the ocean interior has been previously demonstrated, few estimates exist for DOC decay rates within the main thermocline and bathypelagic regions, largely due to the recalcitrant nature of a portion of the exported DOC (Hansell and Carlson, 1998; Carlson, 2002) and the inability of short term bioassays to resolve changes in deep DOC (Barber, 1968). This study demonstrates the utility of combining basin scale observations of DOC variability, water ventilation age and AOU to provide insight to DOC variability and constrain deep DOC decay rates and contribution to AOU.

Acknowledgments

This work was conducted as a component of the US CLIVAR repeat hydrography program, supported by funds from NSF OCE-0752972 to D.A.H and C.A.C. and OCE02241614 and NSF OCE02241614, NSF OCE0648541 and NASA NNX09AL09G to N.B.N., D.S. and C.A.C. Support for WMS is from OCE-0223951. We thank the officers, crew, chief scientists and technicians from the *R.V. Ron Brown* and the *R.V. Knorr*. Conversations with M. Brzezinski, S. Goldberg, C. Swan and C. Nelson and comments from three anonymous reviewers were valuable in the writing of this paper.

References

Alvarez-Salgado, X.A., Nieto-Cid, M., Gago, J., Brea, S., Castro, C.G., Doval, M.D., Perez, F.F., 2006. Stoichiometry of the degradation of dissolved and particulate biogenic organic matter in the NW Iberian upwelling. Journal of Geophysical Research-Oceans 111, C7 art. no. C07017.

Aluwihare, L.I., Repeta, D.J., Chen, R.F., 1997. A major biopolymeric component to dissolved organic carbon in surface sea water. Nature 387, 166–169.

Amon, R., Fitznar, H.P., Benner, R., 2001. Linkage among the bioreactivity, chemical composition and diagenetic state of marine dissolved organic matter. Limnology and Oceanography 46, 287–297.

Amon, R.M.W., Budéus, G., Meon, B., 2003. Dissolved organic carbon distribution and origin in the Nordic Seas: exchanges with the Arctic Ocean and North Atlantic. Journal of Geophysical Research 108, 3221–3238.

Anderson, L.A., 1995. On the hydrogen and oxygen content of marine phytoplankton. Deep-Sea Research I 42, 1675–1680.

Arístegui, J., Agustí, S., Duarte, C.M., 2003. Respiration in the dark ocean. Geophysical Research Letters 30 (2), 1041.

Arístegui, J., Agustí, S., Middelburg, J.J., Duarte, C.M., 2005. Respiration in the mesopelagic and bathypelagic zones of the oceans. In: del Giorgio, P., Williams, P.J.L. (Eds.), Respiration in Aquatic Systems. Oxford Press, Oxford, pp. 181–205.

Arístegui, J., Duarte, C.M., Agustí, S., Doval, M., Alvare-Salgado, A., Hansell, D.A., 2002. Dissolved organic carbon support of respiration in the dark ocean. Science 298, 1967.

Arístegui, J., Gasol, J.M., Duarte, C.M., Herndl, G.J., 2009. Microbial oceanography of the dark ocean's pelagic realm. Limnology and Oceanography 54, 1501–1529.

Azam, F., Fenchel, T., Field, J.G., Gray, J.S., Meyer-Reil, L.A., Thingstad, F., 1983. The ecological role of water-column microbes in the sea. Marine Ecology Progress Series 10, 257–263.

Azam, F., Hodson, R.E., 1977. Size distribution and activity of marine microheterotrophs. Limnology and Oceanography 22, 492–501.

Barber, R.T., 1968. Dissolved organic carbon from deep water resists microbial oxidation. Nature 220, 274–275.

Bauer, J.E., Williams, P.M., Druffel, E.R.M., 1992. ^{14}C activity of dissolved organic carbon fractions in the north-central Pacific and Sargasso Sea. Nature 357, 667–670.

Bauer, J.E., 2002. Carbon Isotopic Composition of DOM. In: Hansell, D.A., Carlson, C.A. (Eds.), Biogeochemistry of Marine Dissolved Organic Matter. Academic Press, San Diego, pp. 405–453.

Bendtsen, J., Lundsgaard, C., Middelboe, M., Archer, D., 2002. Influence of bacterial uptake on deep-ocean dissolved organic carbon. Global Biogeochemical Cycles 16 (4), 1127, doi:10.1029/2002GB001947.

Benner, R., Biddanda, B., 1998. Photochemical transformation of surface and deep marine dissolved organic matter: Effects on bacterial growth. Limnology and Oceanography 43, 1373–1378.

Benner, R.H., 2002. Composition and Reactivity. In: Hansell, D.A., Carlson, C.A. (Eds.), Biogeochemistry of Marine Dissolved Organic Matter. Academic Press, San Diego, pp. 59–90.

Bullister, J.L., Weiss, R.F., 1988. Determination of CCl_3 and CCl_2 F_2 in seawater and air. Deep-Sea Research 35 (1988), 839–853.

Burd, A.B., Hansell, D.A., Steinberg, D.K., Anderson, T.R., Arístegui, J., Baltar, F., Beaupré, S.R., Buesseler, K.O., DeHairs, F., Jackson, G.A., Kadko, D.C., Koppelmann, R., Lampitt, R.S., Nagata, T., Reinthaler, T., Robinson, C., Robison, B.H., Tamburini, C., Tanaka, T., 2010. Assessing the apparent imbalance between geochemical and biochemical indicators of meso- and bathypelagic biological activity: What the @$#! is wrong with present calculation of carbon budgets? Deep-Sea Research II 57 (16), 1557–1571.

Carlson, C.A., 2002. Production and Removal Processes. In: Hansell, D.A., Carlson, C.A. (Eds.), Biogeochemistry of Marine Dissolved Organic Matter. Academic Press, San Diego, pp. 91–151.

Carlson, C.A., Ducklow, H.W., 1996. Growth of bacterioplankton and consumption of dissolved organic carbon in the Sargasso Sea. Aquatic Microbial Ecology 10, 69–85.

Carlson, C.A., Ducklow, H.W., Michaels, A.F., 1994. Annual flux of dissolved organic carbon from the euphotic zone in the northwestern Sargasso Sea. Nature 371, 405–408.

Carlson, C.A., Giovannoni, S.J., Hansell, D.A., Goldberg, S.J., Parsons, R., Vergin, K., 2004. Interactions between DOC, microbial processes, and community structure in the mesopelagic zone of the northwestern Sargasso Sea. Limnology and Oceanography 49, 1073–1083.

Castro, C.G., Nieto-Cid, M., Alvarez-Salgado, X.A., Perez, F.F., 2006. Local remineralization patterns in the mesopelagic zone of the Eastern North Atlantic, off the NW Iberian Peninsula. Deep-Sea Research I 53 (12), 1925–1940.

Cherrier, J., Bauer, J.E., Druffel, E.R.M., 1996. Utilization and turnover of labile dissolved organic matter by bacterial heterotrophs in eastern North Pacific surface waters. Marine Ecology Progress Series 139, 267–279.

Copin-Montégut, G., Avril, B., 1993. Vertical distribution and temporal variation of dissolved organic carbon in the North-Western Mediterranean Sea. Deep-Sea Research I 40 (10), 1963–1972.

Cowie, G.L., Hedges, J.I., 1994. Biochemical indicators of diagenetic alteration in natural organic matter mixtures. Nature 369, 304–307.

Doney, S.C., Bullister, J.L., 1992. A chlorofluorocarbon section in the eastern North Atlantic. Deep-Sea Research I 39 (11–12A), 1857–1883.

Doney, S.C., Jenkins, W.J., Bullister, J.L., 1997. A comparison of ocean tracer dating techniques on a meridional section in the eastern North Atlantic. Deep-Sea Research I 44 (4), 603–626.

Doval, M.D., Hansell, D.A., 2000. Organic carbon and apparent oxygen utilization in the western South Pacific and central Indian Ocean. Marine Chemistry 68, 249–264.

Druffel, E.R.M., Williams, P.M., Bauer, J.E., Ertel, J.R., 1992. Cycling of dissolved and particulate organic matter in the open ocean. Journal of Geophysical Research 97 (C10), 15,639–15,659.

Druffel, E.R.M., Bauer, J.E., Williams, P.M., Griffin, S., Wolgast, D., 1996. Seasonal variability of particulate organic radiocarbon in the northeast Pacific Ocean. Journal of Geophysical Research 101 (C9), 20543–20552.

Druffel, E.R.M., Griffin, S., Bauer, J.E., Wolgast, D.M., Wang, X.-C., 1998. Distribution of particulate organic carbon and radiocarbon in the water column from the upper slope to the abyssal NE Pacific Ocean. Deep-Sea Research II 45, 667–687.

Druffel, E.R.M., Williams, P.M., 1990. Identification of a deep marine source of particulate organic carbon using bomb 14C. Nature 347, 172–174.

Druffel, E.R.M., Williams, P.M., Robertson, K., Griffin, S., Jull, A.J.T., Donahue, D., Toolin, L., Linick, T.W., 1989. Radiocarbon in dissolved organic and inorganic carbon from the central north Pacific. Radiocarbon 31, 523–532.

Ducklow, H.W., Carlson, C.A., Bates, N.R., Knap, A.H., Michaels, A.F., 1995. Dissolved organic carbon as a component of the biological pump in the North Atlantic Ocean. Philisophical Transactions of the Royal Society, Series A 348, 161–167.

Engel, A., Thoms, S., Riabesell, U., Rochell-Newall, E., Zondervan, I., 2004. Polysaccharide aggregation as a potential sink of marine dissolved organic carbon. Nature 428, 929–932.
Feely, R.A., Talley, L.D., Johnson, G.C., Sabine, C.L., Wannikhof, R., 2005. Repeat hydrography cruises reveal chemical changes in the North Atlantic. EOS Transactions of American Geophysical Union 86 (399), 404–405.
Fine, R.A., Rhein, M., Andrie, C., 2002. Using a CFC effective age to estimate propagation and storage of climate anomalies in the deep western North Atlantic Ocean. Geophysical Research Letters 29 (24), 2227–2230.
Goldberg, S.J., Carlson, C.A., Hansell, D.A., Nelson, N.B., Siegel, D.A., 2009. Temporal dynamics of dissolved combined neutral sugars and the quality of dissolved organic matter in the Northwestern Sargasso Sea. Deep-Sea Research I 56, 672–685.
Gruber, N., Sarmiento, J.L., 1997. Global patterns of marine nitrogen fixation and denitrification. Global Biogeochemical Cycles 11 (2), 235–266.
Guo, L., Coleman, C.H., Santschi, P.H., 1994. The distribution of colloidal and dissolved organic carbon in the Gulf of Mexico. Marine Chemistry 45, 105–119.
Haine, T.W.N., Richards, K.J., 1995. The influence of the seasonal mixed layer on oceanic uptake of CFCs. Journal of Geophysical Research 100, 10727–10744.
Haine, T.W.N., Richards, K.J., Jia, Y.L., 2003. Chlorofluorocarbon constraints on North Atlantic ventilation. Journal of Physical Oceanography 33 (8), 1798–1814.
Hansell, D.A., 2002. DOC in the Global Ocean Carbon Cycle. In: Hansell, D.A., Carlson, C.A. (Eds.), Biogeochemistry of Marine Dissolved Organic Matter. Academic Press, San Diego, pp. 685–716.
Hansell, D.A., Bates, N.R., Olson, D.B., 2004. Excess nitrate and nitrogen fixation in the North Atlantic Ocean. Marine Chemistry 84, 243–265.
Hansell, D.A., Carlson, C.A., 1998. Deep ocean gradients in dissolved organic carbon concentrations. Nature 395, 263–266.
Hansell, D.A., Carlson, C.A., 2001a. Biogeochemistry of total organic carbon and nitrogen in the Sargasso Sea: control by convective overturn. Deep-Sea Research II 48, 1649–1667.
Hansell, D.A., Carlson, C.A., 2001b. Marine dissolved organic matter and the carbon cycle. Oceanography 14, 41–49.
Hansell, D.A., Carlson, C.A., Repeta, D.J., Shlitzer, R., 2009. Dissolved organic matter in the ocean: new insights stimulated by a controversy. Oceanography in press.
Hansell, D.A., Carlson, C.A., Suzuki, Y., 2002. Dissolved organic carbon export with North Pacific intermediate water formation. Global Biogeochemical Cycles 16, 77–84.
Hansell, D.A., Olson, D.B., Dentener, F., Zamora, L.M., 2007. Assessment of excess nitrate development in the subtropical North Atlantic. Marine Chemistry 106, 562–579.
Hansman, R.L., Griffin, S., Watson, J.T., Druffel, E.R., Ingalls, A.E., Pearson, A., Aluwihare, L.I., 2009. The radiocarbon signature of microorganisms in the mesopelagic ocean. Proceedings of the National Academy of Science 106 (16), 6513–6518.
Holzer, M., Hall, T.M., 2000. Transit-time and tracer-age distributions in geophysical flows. Journal of Atmospheric Science 57, 3539–3558.
Hopkinson, C.S., Vallino, J.J., 2005. Efficient export of carbon to the deep ocean through dissolved organic matter. Nature 433 (7022), 142–145.
Herndl, G.J., Reinthaler, T., Teira, E., van Aken, H., Veth, C., Pernthaler, A., Pernthaler, J., 2005. Contribution of Archaea to total prokaryotic production in the deep Atlantic Ocean. Applied and Environmental Microbiology 71 (5), 2303–2309.
Ingalls, A.E., Shah, S.R., Hansman, R.L., Aluwihare, L.I., Santos, G.M., Druffel, E.R.M., Pearson, A., 2006. Quantifying archaeal community autotrophy in the mesopelagic ocean using natural radiocarbon. Proceedings of the National Academy of Sciences of the United States of America 103 (17), 6442–6447.
Joyce, T.M., Hernandez-Guerra, A., Smethie, W.M., 2001. Zonal circulation in the NW Atlantic and Caribbean from a meridional World Ocean Circulation experiment hydrographic section at 66°W. Journal of Geophysical Research 106 (C10), 22,095–22,114.
Kähler, P., Koeve, W., 2001. Dissolved organic matter in the sea: can its C:N ratio explain carbon overconsumption? Deep-Sea Research I 48 49–62.
Khatiwala, S., Visbeck, M., Schlosser, P., 2001. Age tracers in an ocean GCM. Deep-Sea Research I 48, 1423–1441.
Khatiwala, S., 2007. A conceptual framework for simulation of a biogeochemical tracers in the ocean. Global Biogeochemical Cycles 21, 2923–2937.
Khatiwala, S., Hall, T.M., Primeau, F., 2009. Reconstruction of the history of anthropogenic CO_2 in the ocean over the industrial era. Nature 462, doi:10.1038/nature08526.
Lee, K., 2001. Global net community production estimated from the annual cycle of surface water total dissolved inorganic carbon. Limnology and Oceanography 46 (6), 1287–1297.
Louanchi, F., Najjar, R.G., 2001. Annual cycles of nutrients and oxygen in the upper layers of the North Atlantic Ocean. Deep-Sea Research II 48 (10), 2155–2171.
Meador, T.B., Gogou, A., Spyres, G., Herndl, G.J., Krasakopoulou, E., Psarra, S., Yokokawa, T., DeCorte, D., Zervakis, V., Repeta, D.J., 2010. Biogeochemical relationships between ultrafiltered dissolved organic matter and picoplankton activity in the Eastern Mediterranean Sea. Deep-Sea Research II 57 (16), 1460–1477.
Menzel, D.W., 1964. The distribution of dissolved organic carbon in the Western Indian Ocean. Deep-Sea Research 11, 757–765.
Mopper, K., Kieber, D.J., 2002. Photochemistry and cycling of carbon, sulfur, nitrogen and phosphorus. In: Hansell, D.A., Carlson, C.A. (Eds.), Biogeochemistry of Marine Dissolved Organic Matter. Academic Press, San Diego, pp. 456–508.
Nelson, N.B., Siegel, D.A., Carlson, C.A., Swan, C., Smethie, W.M., Khatiwala, S., 2007. Hydrography of chromophoric dissolved organic matter in the North Atlantic. Deep-Sea Research I 54 (5), 710–731.
Ogura, N., 1970. The relation between dissolved organic carbon and apparent oxygen utilization in the Western North Pacific. Deep-Sea Research 17, 221–231.
Passow, U., Alldredge, A.L., 1994. Distribution, size and bacterial colonization of transparent exopolymer particles (TEP) in the ocean. Marine Ecology Progress Series 113, 185–198.
Peltzer, E.T., Hayward, N.A., 1996. Spatial distribution and temporal variability of total organic carbon along 140°W in the equatorial Pacific Ocean in 1992. Deep-Sea Research II 43, 1155–1180.
Reinthaler, T., van Aken, H., Veth, C., Arístegui, J., Robinson, C., Williams, P., Lebaron, P., Herndl, G.J., 2006. Prokaryotic respiration and production in the meso- and bathypelagic realm of the eastern and western North Atlantic basin. Limnology and Oceanography 51 (3), 1262–1273.
Reinthaler, T., vanAken, H.M., Herndl, G.J., 2010. Major contribution of autotrophy to microbial carbon cycling in the deep North Atlantic interior. Deep-Sea Research II 57 (16), 1572–1580.
Robinson, C., Steinberg, D.K., Koppelmann, R., Robison, B.H., Anderson, T.R., Arístegui, J., Carlson, C.A., Frost, J.R., Ghiglione, J.F., Hernández-León, S., Jackson, G.A., Quéguiner, B., Ragueneau, O., Rassoulzadegan, F., Tamburini, C., Tanaka, R., Wishner, K.F., Zhang, J., 2010. Mesopelagic zone ecology and biogeochemistry - a synthesis. Deep-Sea Research II 57 (16), 1504–1518.
Santinelli, C., Nannicini, L., Seritti, A., 2010. DOC dynamics in meso- and bathypelagic layers of the Mediterranean Sea. Deep-Sea Research II 57 (16), 1446–1459.
Schneider, B., Karstensen, J., Oschlies, A., 2005. Model-based evaluation of methods to determine C:N and N:P regeneration ratios from dissolved nutrients. Global Biogeochemical Cycles, 19.
Schlitzer, R., 2000. Applying the adjoint method for global biogeochemical modeling. In: Kasibhatla, P., Heimann, M., Hartley, D., Mahowald, N., Prinn, R., Rayner, P. (Eds.), Inverse Methods in Global Biogeochemical Cycles. AGU Geophysical Monograph Series, pp. 107–124.
Schlitzer, R., 2004. Ocean Data View. 〈http://www.awi-bremerhaven.de/GEO/ODV/〉.
Schmitz, W.J., 1996. On the World Ocean Circulation: Volume II. Technical Report WHOI-96-08. Woods Hole Oceanographic Institutioin, Woods Hole, MA, p. 237.
Schmitz, W.J., Richardson, P.L., 1991. On the sources of the Florida Current. Deep-Sea Research 38 (Suppl. 1), S389–S409.
Sharp, J.H., Carlson, C.A., Peltzer, E.T., Castle-Ward, D.M., Savidge, K.B., Rinker, K.R., 2002. Final dissolved organic carbon broad community intercalibration and preliminary use of DOC reference materials. Marine Chemistry 77 (4), 239–253.
Shiah, F.K., Ducklow, H.W., 1994. Temperature and substrate regulation of bacterial abundance, production and specific growth rate in Chesapeake Bay, USA. Marine Ecology Progress Series 103, 297–308.
Skoog, A., Benner, R., 1997. Aldoses in various size fractions of marine organic matter: Implications for carbon cycling. Limnology and Oceanography 42 (8), 1803–1813.
Smethie, W.M., Fine, R.A., 2001. Rates of North Atlantic Deep Water formation calculated from chlorofluorocarbon inventories. Deep-Sea Research I 48 (1), 189–215.
Smethie, W.M., Fine, R.A., Putzka, A., Jones, E.P., 2000. Tracing the flow of North Atlantic Deep Water using chlorofluorocarbons. Journal of Geophysical Research-Oceans 105 (C6), 14297–14323.
Sohrin, R., Sempere, R., 2005. Seasonal variation in total organic carbon in the northeast Atlantic in 2000-2001. Journal of Geophysical Research-Oceans 110 (C10).
Steinberg, D.K., Van Mooy, B.A.S., Buesseler, K.O., Boyd, P.W., Kobari, T., Karl, D.M., 2008. Bacterial vs. zooplankton control of sinking particle flux in the ocean's twilight zone. Limnology and Oceanography 53, 1327–1338.
Takahashi, T., Broecker, W.S., Langer, S., 1985. Redfield ratio based on chemical data from isopycnal surfaces. Journal of Geophysical Research 90, 6907–6924.
Teira, E., van Aken, H., Veth, C., Herndl, G.J., 2006. Archaeal uptake of enantiomeric amino acids in the meso- and bathypelagic waters of the North Atlantic. Limnology and Oceanography 51 (1), 60–69.
Tian, R.C., Deibel, D., Rivkin, R.B., Vézina, A.F., 2004. Biogenic carbon and nitrogen export in a deep-convection region. Simulation in the Labrador Sea. Deep-Sea Research I 51, 413–437.
Verdugo, P., Alldredge, A., Azam, F., Kirchman, D.L., Passow, U., Santschi, P.H., 2004. The oceanic gel phase: a bridge in the DOM-POM continuum. Marine Chemistry 92, 67–85.
Verdugo, P. and Santschi, P.H., 2010. Polymer dynamics of DOC networks and gel formation in seawater. Deep-Sea Research II 57 (16), 1486–1493.
Walker, S.J., Weiss, R.F., Salameh, P.K., 2000. Reconstructed histories of the annual mean atmospheric mole fractions for the halocarbons CFC-11, CFC-12, CFC-113, and carbon tetrachloride. Journal of Geophysical Research-Oceans 105 (C6), 14285–14296.
Warner, M.J., Weiss, R.F., 1985. Solubilities of chlorofluorocarbons 11 and 12 in water and seawater. Deep-Sea Research Part A 32 (12), 1485–1497.
Waugh, D.W., Hanie, T.W.N., Hall, T.M., 2004. Transport times and anthropogenic carbon in the subpolar North Atlantic Ocean. Deep-Sea Research I 51, 1475–1491.
Wells, M.L., 1998. Marine colloids: A neglected dimension. Nature 391, 530–531.

Williams, P.J.l, 1981. Incorporation of microheterotrophic processes into the classical paradigm of the planktonic food web. Kieler Meeresforsch 5, 1–28.

Williams, P.J.l, 2000. Heterotrophic bacteria and the dynamics of dissolved organic material. In: Kirchman, D.L. (Ed.), Microbial Ecology of the Oceans. Wiley-Liss, New York, pp. 153–200 pp.

WOCE operations manual. 1994 WOCE Hydrographic Program Office Rep. WHPO 91-1, WOCE Rep. 68/91 〈http://www.jodc.go.jp/JGOFS_DMO/testpage/Publications/WOCE/woce_whp91-1l.htm〉.

Zweifel, U.L., Norrman, B., Hagström, Å, 1993. Consumption of dissolved organic carbon by marine bacteria and demand for inorganic nutrients. Marine Ecology Progress Series 101, 23–32.